University of Baghdad
College of Engineering
JE
JOURNAL OF ENGINEERING

Journal of Engineering
journal homepage: www.joe.uobaghdad.edu.iq
Number 11 Volume 26 November 2020

Civil and Architectural Engineering

Nonlinear Finite Element Analysis of RCMD Beams with Large Circular Opening Strengthened with CFRP Material

Aya waleed Naqe
M.Sc. Student
Department of Civil Engineering, University of Baghdad,
Baghdad, Iraq,
E-mail: ayawaleed971@gmail.com

Dr. Alaa H. Al-zuhairi
Assist. Professor
Department of Civil Engineering, University of Baghdad,
Baghdad, Iraq,
E-mail: alaalwn@coeng.uobaghdad.edu.iq

ABSTRACT

This paper presents the non-linear finite element method to study the behavior of four reinforced rectangular concrete MD beams with web circular openings tested under two-point load. The numerical finite elements methods have been used in a much more practical way to achieve approximate solutions for more complex problems. The ABAQUS /CAE is chosen to explore the behavior of MD beams. This paper also studies, the effect of both size and shape of the circular apertures of MD beams. The strengthening technique that used in this paper is externally strengthening using CFRP around the opening in the MD beams. The numerical results were compared to the experimental results in terms of ultimate load failure and displacement. The FE results showed a good agreement with experimental results.

Keywords: Concrete beams, circle opening, strengthening, finite element method.

التحليل الاخطي للعتبات الخرسانية معتدلة العمق المسلحة ذات الفتحات الدائرية الكبيرة المقواة بمادة الياف الكاربون البوليمرية

أ.م.د علاء حسين الزهيري
قسم الهندسة المدنية - كلية الهندسة - جامعة بغداد

اية وليد نقي
قسم الهندسة المدنية - كلية الهندسة - جامعة بغداد

الخلاصة

يقدم هذا البحث طريقة العناصر المحدودة غير الخطية لدراسة أربعة عتبات خرسانية مستطيلة معتدلة العمق مع فتحات دائرية اختبرت تحت حمل نقطتين .تم استخدام الطرق العددية مثل العناصر المحدودة بطريقة أكثر عملية لتحقيق حلول تقريبية لمشاكل أكثر تعقيدًا .يتم اختيار ABAQUS / CAE لاستكشاف سلوك العتبات. يدرس هذة البحث أيضًا حجم وشكل الفتحة في العتبات معتدلة العمق. تقنية التقوية المستخدمة في هذا البحث هية التقوية الخارجية باستخدام CFRP حول الفتحات في العتبات معتدلة

*Corresponding author
Peer review under the responsibility of University of Baghdad.
https://doi.org/10.31026/j.eng.2020.11.11

Article received: 19/5/2020
Article accepted:30/6/2020
Article published:1/11/2020

العمق. تمت مقارنة النتائج العددية بالنتائج التجريبية من حيث فشل الحمل النهائي والإزاحة. أظهرت نتائج FE توافقًا جيدًا مع النتائج التجريبية.

الكلمات الرئيسية: عتبات خرسانية ، فتحات دائرية ، تقوية ، طريقة العناصر المحدودة.

1. INTRODUCTION

The RCMD become important in the building materials and widely used in engineering structures. There are many practical problems in the RC have to be solved by modern analytical methods, either highly difficult or impossible. Problems related to the representation of the boundary conditions and load or some of the constitutive relationships of stress-strain, the method roughly approximates the unknown domain function. The broad structure is subdivided into smaller, simpler sections called FE. The equations used to model these FE put together in system have a larger equation that used to model all problems. In this research, the efforts of many researchers who studied the behavior of beams with opening strengthened with CFRP material. Mansur et. al. **(Mansur ،2006)** study RC T-beams with small opening strengthening with FRP plates. K. Senthil (K. Senthil2018) study the behavior of six concrete deep beam that opening subjected to static monotonic loading by using finite element program ABAQUS/CAE in addition to that, seventeen beams were simulated under static loading with different shape, size and location opening of deep beam and the result show that the deep beam which having a circle opening undergo lesser the deflection. Abdalla et.al. **(Abdalla ،2003)** study the behavior of RC beams with rectangular opening with shear strengthening using FRP sheets. Ali Hussein (Al-Ahmed, 2016) investigate the behavior of reinforced concrete RC deep beams strengthened with CFRP strips. Maaddawy and Sherif **(Sherif ،Jun. 2009)** investigated the use of FRP sheets for shear strengthening of deep concrete beams with square openings.

2. MATERIALS PROPERTIES

Ordinary Portland cement (type I) was utilized for all the mixes and It was produced by The United Cement Company (Tasluja-Bazian) in Al-Sulaymaniyah / Iraq (IQ.S.No40, 1984). Fine aggregate (zone 2) and coarse aggregate (maximum size19 mm) were used according to (IQ.S. No45, 1980) as showing in **Figs. 1** The fine and coarse aggregate has specific gravity 2.65 and 2.63, respectively. Four sizes of steel reinforcing bars were used in the tested beams, deformed bars of size (Ø16) mm and (Ø10) mm were used as longitudinal reinforcement, and deformed steel bars of size (Ø 8) mm were used as closed stirrups and bar size (Ø12) mm for diagonal reinforcement. The superplasticizer was Supaflo (PC200) High-performance and super plasticization admixture of poly-carboxylic polymers ether with long chains was used as plasticizing agent add to concrete mixes. ((PC200), 2014). For externally strengthening use carbon fiber CFRP fabric known as Sika Wrap-900c in this study as showing in **Figs. 2** (CFRP, 2017).

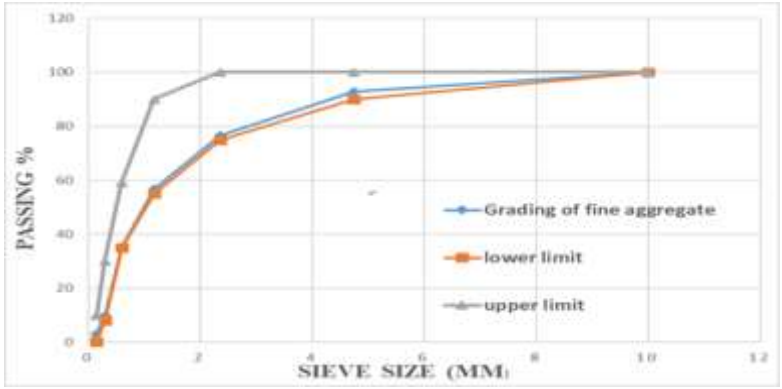

a. fine aggregate

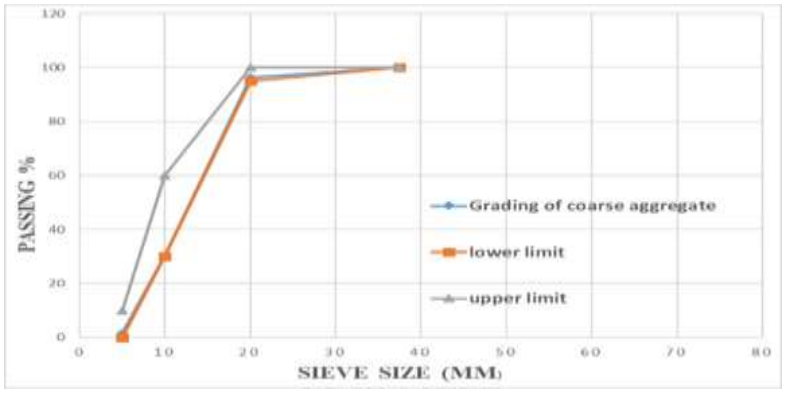

b. coarse aggregate

Figure1. Specification limits of aggregate.

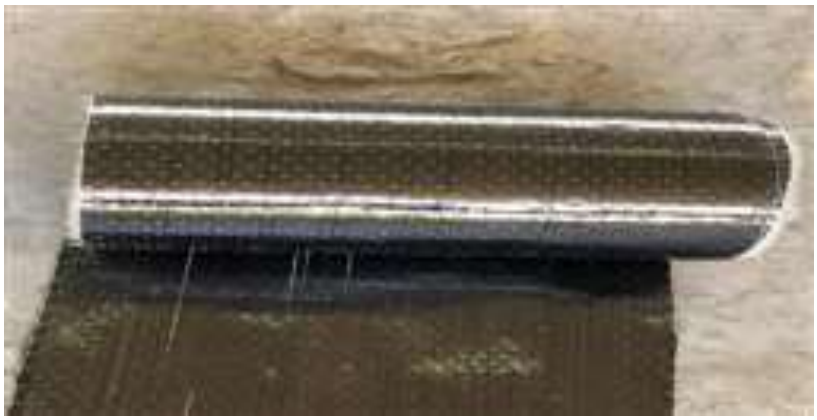

Figure 2. (CFRP) Sika wrap-900c.

3. CONCRETE MIX DESIGN

The concrete mixture was design using (ACI) method to obtain the concrete mix constituents that achieves strength of 30 MPa. The concrete mix is designed depending on the strength of concrete according the requirement of the ACI code **(ACI 318, 2014)** was adopted to get a suitable concrete mix permitting to the test result of sand and gravel The final mix used is showing in **Table 1.**

Table 1. Concrete mix design.

For 1 m^3 of concrete	Cement (Kg)	Sand (Kg)	Gravel (Kg)	Water (L)	Superplasticizer (L)
	380	850	1005	165	5

4.ANALYSIS COMPUTER SOFTWARE(ABAQUS)

4.1 Constitutive Model of Reinforcing Bar Steel

The steel deformation causes only elastic stresses before reaching the yield point, which is recovered at all with the removal of the applied load. However, when the steel pressure exceeds the yield stress, plastic deformation occurs. In the post-production region, both elastic a plastic stresses accumulate as the metal deforms as showing in (Table 2), when the material yields the stiffness of the steel decrease. For subsequent loadings, the plastic deformation of the steel material's raises its yield stress. The material properties of the plate steel and the supporting gigue is shown in (Table 3), and identical values are considered to those for longitudinal bars.

Table 2. Elastic and plastic input data for rebar.

Elastic	Young's modulus of elasticity		200000 MPa
	Poisson's ratio ν		0.3
Density	Mass Density		7.85*10^9
Plastic	Ø	Yield Stress	Plastic Strain
	8	392.52	0
		589.97	0.153
	10	600.25	0
		693.25	0.117
	12	578.91	0
		686.48	0.15
	16	576.68	0
		673.22	0.153

Table 3. Elastic input data for steel plate.

Elastic	Young's modulus of elasticity	400000 MPa
	Poisson's ratio ν	0.3
Density	Mass Density	7.85*10^9
Plastic	Yield Stress	700
	Plastic Strain	0

4.1 Constitutive Model of Concrete

In this research, the linear used for elastic and the nonlinear used for damaged plasticity model because both states show low deformability in concrete. The elastic stiffness induced by the plastic straining both in tension and compression in the material constitutive model as show in **Table 4.**

Table 4. Input data for concrete.

Elastic	Young's modulus of elasticity	26000 MPa
	Poisson's ratio ν	0.18
Density	Mass Density	2.5*10^9
Density	Mass Density	2.5*10^9

4.2 Concrete Damaged Plasticity Model

In the concrete damaged plasticity model, the total strain tensor ε was comprised of the elastic part ε^{el} and the plastic part ε^{pl} (**Hejazi, 05 June 2017**).

$$\varepsilon = \varepsilon^{el} + \varepsilon^{pl} \quad (1)$$

$$\sigma = D^{el}: (\varepsilon - \varepsilon^{pl}) \quad (2)$$

$$\bar{\sigma} = D_0{}^{el}: (\varepsilon - \varepsilon^{pl}) \quad (3)$$

$$D^{el} = (1 - d)\, D_0^{el} \quad (4)$$

The nominal stress with the elastic tensor degraded from (4) could be rewritten as follows:

$$\sigma = (1 - d)\, D_0^{el} : (\varepsilon - \varepsilon^{pl}) \quad (5)$$

The constitutive damage plasticity model was based on the following stress – strain relationship:

$$\sigma = (1 - d)\, \bar{\sigma} \rightarrow (1 - d_t)\bar{\sigma}_t + (1 - d_c)\, \bar{\sigma}_c \quad (6)$$

Where d_t and d_c were two variables of scalar damage, ranging from 0 (undamaged) to 1 (well damaged). The harm model used for concrete was based on plasticity and called the tensile cracking and compressive crushing process failure. At first the stress-strain relationship under uniaxial tension is linearly elastic until the value of the failure stress is reached. Failure stresses are modified in the concrete block to remove micro-cracks within it. Beyond the tension of failure in concrete terms, Response to stress-strain is built with softening properties **Figs. 3b**. Under uniaxial compression the response is linear until the initial yield value is reached. After the ultimate tension in the plastic zone has been achieved, concrete reaction is defined by stress hardening accompanied by strain-softening **Figs. 3a**.

Figs. 3 Stated that the compressive uniaxial and tensile concrete response are assumed to be impaired by damaged plasticity; and that assumption forms the model's basis. The tensile reactions and uniaxial compressive of concrete were provided in relation to the plasticity model of concrete damage subjected to tension and compression load gave:

$$\sigma_t = (1 - d_t)\, E_0(\varepsilon_t - \varepsilon_t^{pl,h}) \quad (7)$$

$$\sigma_c = (1 - d_c)\, E_0(\varepsilon_c - \varepsilon_c^{pl,h}) \quad (8)$$

Given the nominal uniaxial stress, the effective uniaxial stress $\bar{\sigma}_t$ and $\bar{\sigma}_c$ were derived as follows:

$$\bar{\sigma}_t = \frac{\sigma_t}{(1 - d_t)} = E_0(\varepsilon_t - \varepsilon_t^{pl,h}) \quad (9)$$

$$\bar{\sigma}_c = \frac{\sigma_c}{(1 - d_c)} = E_0(\varepsilon_c - \varepsilon_c^{pl,h}) \quad (10)$$

where compressive strain ε_c equaled $\varepsilon_c^{pl,h} + \varepsilon_c^{el}$, and tensile strain ε_t equalled $\varepsilon_t^{pl,h}t + \varepsilon_t^{el}$.

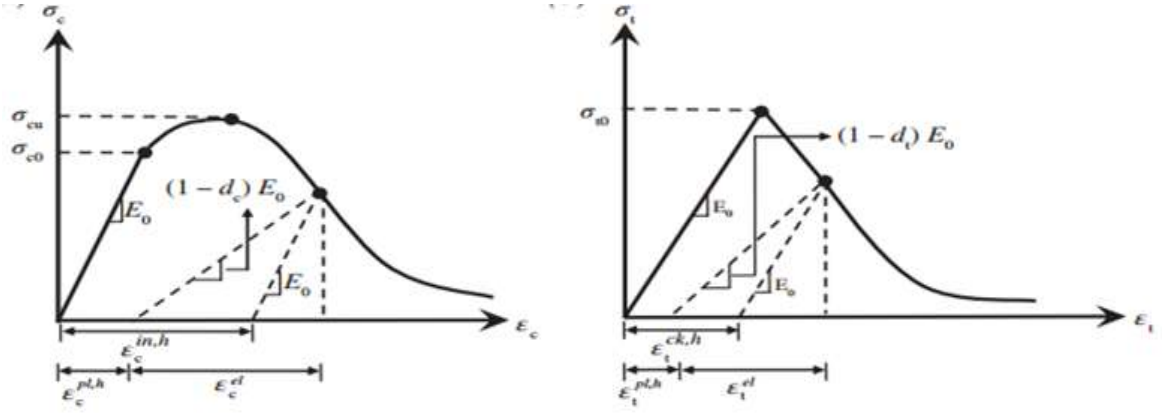

(a). Compression (b). Tension

Figure 3. Response of concrete to a uniaxial loading condition.

4.3 Plasticity parameters

The model of concrete passes through two steps. The first one is an elastic model in which the Poisson's ratio was defined and the second one the damage plasticity model was adopted to define the nonlinear portion of the stress-strain curve of the concrete. The plasticity has a five parameters must be defined to solve the plastic flow and yield function see **Table 5. (Abaqus2017-2016 ،)**.

Table 5. The parameters plastic properties used in tested beam.

Plasticity parameters	
Dilation angle	30
Eccentricity	0.1
f_{b0}/f_{c0}	1.16
Viscosity parameter	0.667
$k_c$parameters	0.0001

4.4 Carbon fiber reinforced polymer (CFRP)

Carbon fiber reinforced polymer (CFRP) has been used as an excellent material in strengthening or retrofitting existing structures such as beams, columns, and slabs. This use has become popular worldwide due to superior properties of CFRP materials. the thickness of this type of CFRP is 0.478 used in this search. The values shown in (Table 6) for CFRP were obtained from the CFRP Properties sheet **(CFRP, 2017).**

Table 6. CFRP input data for lamina.

density	1810	
elastic	Yong modulus	242000 GPa or MPa
	Passion ratio	0.3
lamina	E1	117333
	E2	10544
	Nu12	0.3
	G13	5582
	G12	5582
	G23	3538.2

4.5 Hashin damage for fiber

The Hashin damage model expects anisotropic damage to fragile-elastic materials. It is designed mainly for use of fiber-reinforced composite materials and takes into consideration four different modes of failure: matrix compression, fiber tension, matrix strain, and fiber compression. Which are criteria for integrating failure, where more than one stress factor was used to test the various failure types

5. SPECIMENS

For all test MD beams, four reinforced concrete beams with 8 mm stirrups and spaced at 50 (mm) from the end of each beam and a concrete cover of 15 (mm) were used. The longitudinal flexural tensile reinforcement is (4 Ø 16) deformed steel bars, the longitudinal compression reinforcement is (2 Ø 10) deformed steel bars. While the vertical shear reinforcement (stirrups) is design with (Ø8 @ 140 (mm) as showing in **Table 7. (ACI318, 2014).** While, Support plates used to cover beams

have measurements of 250 x 100 x 30 (mm). The type of opening is circular with a diameter of 110,160, and 225 (mm) (Maryam Abdul Jabbar Hassan, 5, 2019) and these openings were placed in different location of shear span and in numbers two, four and eight respectively. The detailing of beams shows in **Figs.(4to7)**. The beams strengthened by one layer of CFRP strips with a constant width 30,40, and 50(mm) for top chord, bottom chord and for vertical column respectively were chosen carefully based on the failure mode of the reference beams **(Shammari, 23 October 2015).**

Table 7. The steel reinforcement detail.

Specimen symbols	Main Rebar details	Transverse Rebar details	stirrups
C.B	4Q16	2Q10	Q8@140mm
RCBCO,1	4Q16	3Q12	Q8@140mm
RCBCO,2	4Q16	2Q10	Q8@160mm
RCBCO,4	4Q16	2Q10	Q8@150mm

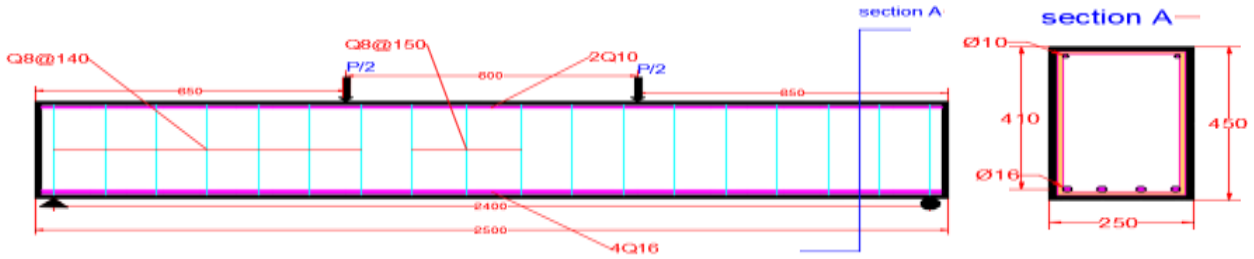

Figure 4. Detailing of Controlled Beam.

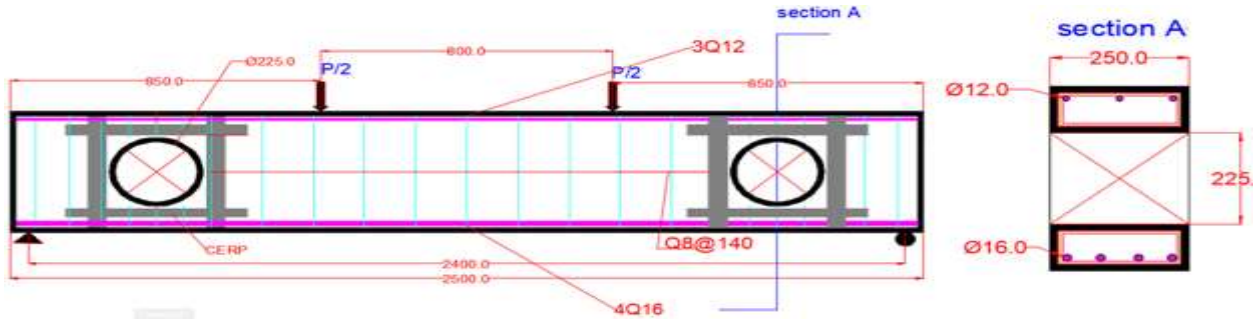

Figure 5. Detailing of beam with two circler opening strengthened with CFRP.

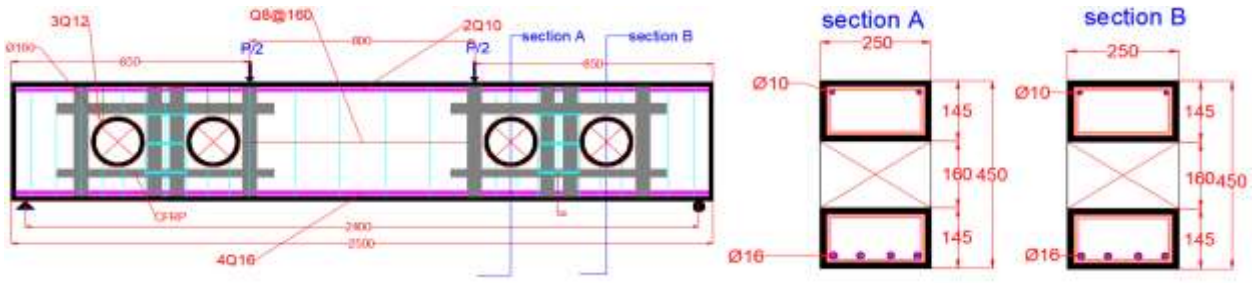

Figure 6. Detailing of beam with four circler opening strengthened with CFRP.

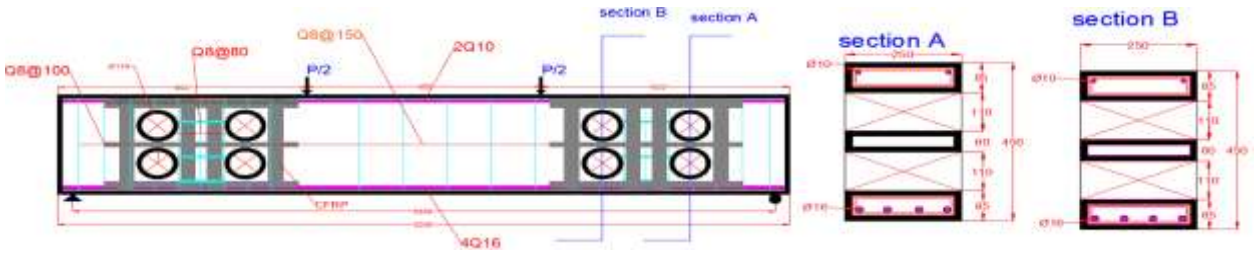

Figure 7. Detailing of beam with eight circler opening strengthened with CFRP.

6. MODELING OF BEAMS IN FINITE ELEMENT

There are two integration rules that used in ABAQUS, the first rule is the reduced Gauss-quadrature integration 8(2x2x2) and the second rule is the full Gauss-quadrature integration 27(3x3x3). (Abaqus, 2016-2017). for concrete used the three dimensional twenty -node linear brick element with reduced integration and hourglass control (C3D20R) (Ahmed2014 ،). Which the(C3D20) element is a general-purpose quadratic brick element (3x3x3 integration points). However, several types of three-dimensional of The node numbering follows the convention is shown in **Figs.(8a)** and the integration scheme is given in **Figs.(8b)**. Also in this study the reinforced bar has been modeled a truss element liner (T3D2) as axial members (A 2-node linear 3D truss element) embedded within the concrete element, perfect bond occurs between the steel bars and the concrete as shown in **Figs. 9** (Al-Ahmed, 2016). Simulation of the bearing plates at the bottom of the specimen using quadratic elements (full touch element with the complete connection between the bearing plates and the specimen) and for the CFRP is defined as Shell elements (S8R) were employed to represent, the S8R element has six degrees of freedom per node. This type of element was commonly used to model this kind of contact zone, see **Figs. 10**.

(**a).** 20-node brick eleme (**b).**3x3x3 integration point scheme in hexahedral elements

Figure 8. The C3D20 element of concrete.

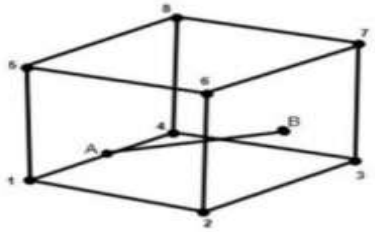

Figure 9. Truss element AB embedded in (3-D) continuum element node A is constrained to edge 1-4and node B is constrained to face2-6-7-3 (Jassim, 2017).

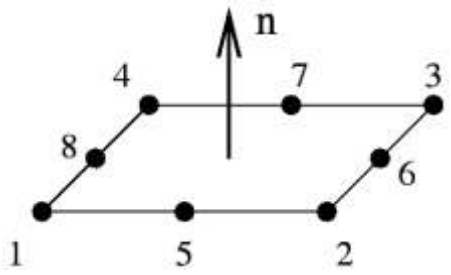

Figure 10. 8-node quadratic element of CFRP.

7. MODELING METHODOLOGY

The load applied as displacement on the top of the bearing plate surface (250 ,100) mm The applied boundary support and loading conditions are shown in **Figs. 11.** And for the support Modeling borders properly in ABAQUS / Standard is considered one of the most complex aspects of the process (Abaqus, 2016-2017). The supporting condition has been modeled in the beams segments as Encastre ux=uy=uz=UR1=UR2==UR30 support. The interaction between the steel plate which defined as rigid body and the load which need a coupling tie between the reference point and the plate to determine the load. The model is divided (meshed) into a number of small elements (Dr. Rafa'a Mahmood Abbas, March 2015), and after loading, stresses and strains are calculated at integration points of these small elements (S.C. Chin, 2012), **Figs. (12)**. The 3D FE meshes were adopted for the specimens.

Figure 11. Loadings and Boundary Conditions of the tested beam.

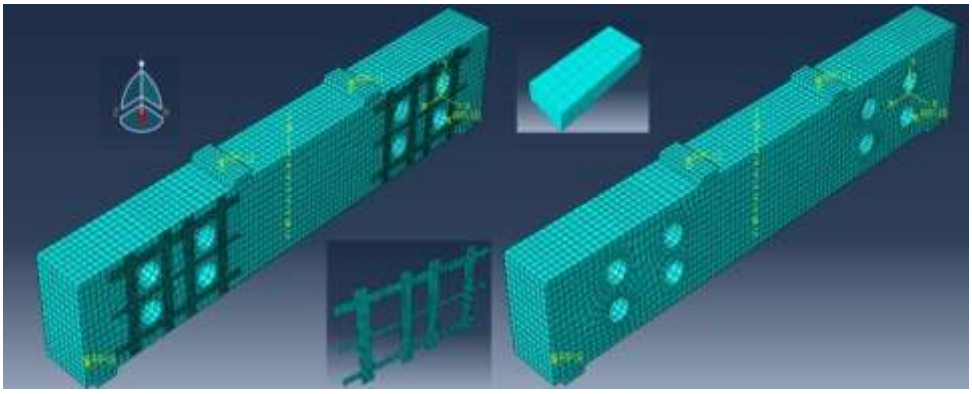

Figure 12. mashing of beam.

8. DYNAMIC AND QUASI-STATIC FAILURE CRITERIA FOR CONCRETE

The suggested method for modeling material damage and failure at ABAQUS is incremental damage and failure models described in The harm and failure of ductile metals These models are ideal for both quasi-static conditions and complex ones. ABAQUS Specific provides two additional types of system loss appropriate only for complex high strength issues. The action of concrete under quasi-static loads for uniaxial loading, friction and plane stress conditions is

observed. The loss conditions for concrete are discussed as well as the techniques for the definition of constitutive parameters. The emphasis is on an enthusiastic understanding of the defined failure criterion.

9. ULTIMATE LOADS AND MAXIMUM DEFLECTIONS

(Table 7) reports the ultimate loads and cumulative deflections for both experimentally evaluated MD beams and FEM. The final loads of the FEM are the last steps load applied before the solution starts to diverge due to several fractures and large deflections. **Table 8.** also show the difference between the FE and the experiment MD beams, these difference backs to the Micro-cracks reduce the stiffness of the beam and produce duo to shrinkage of the concrete and the FE do not include theses micro-cracks.

Table 8. Comparisons of failure load and maximum deflection.

Ultimate Load (Pu)					
Beam	EXP (kN)	F.E.M (kN)	Decreasing percentage %	Difference, (%)	FE/EXP
Solid beam	350	369.226	……	5.5	1.05
RCBCO,2	180	198.36	48.57	10.2	1.10
RCBCO,4	270	281.49	22.8	4.2	1.04
RCBCO,8	250	260.282	28.5	4.1	1.04
Maximum Deflection (Δmax)					
Beam	EXP (mm)	F.E.M (mm)	FE/EXP		
Solid beam	7.12	6.07	0.85		
RCBCO,2	5.11	3.8	0.74		
RCBCO,4	6.32	5	0.79		
RCBCO,8	5.32	4.5	0.84		

10. LOAD-DEFLECTION CURVES

As the experimentally tested beams, deflections (Vertical displacements) were recorded at mid-span at the center of the bottom face of the FEM in y-direction (UY2) (Abaqus2017-2016 ،). There is a reasonable agreement between FEA results and experimental results. Contour deflection plots for all beams subjected to static load at the last load stage are shown in **Figs. 13**. and the comparison of experimental of mid-span- load deflection with ABAQUS are shown in **Figs. 14**.

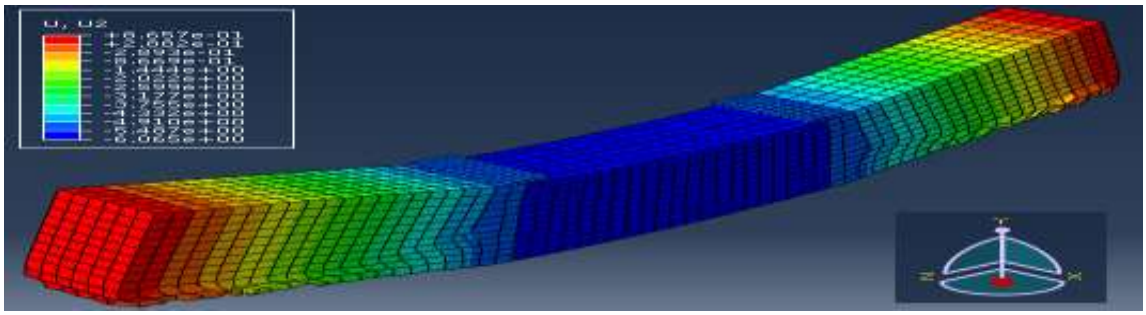

(a). solid MD beam

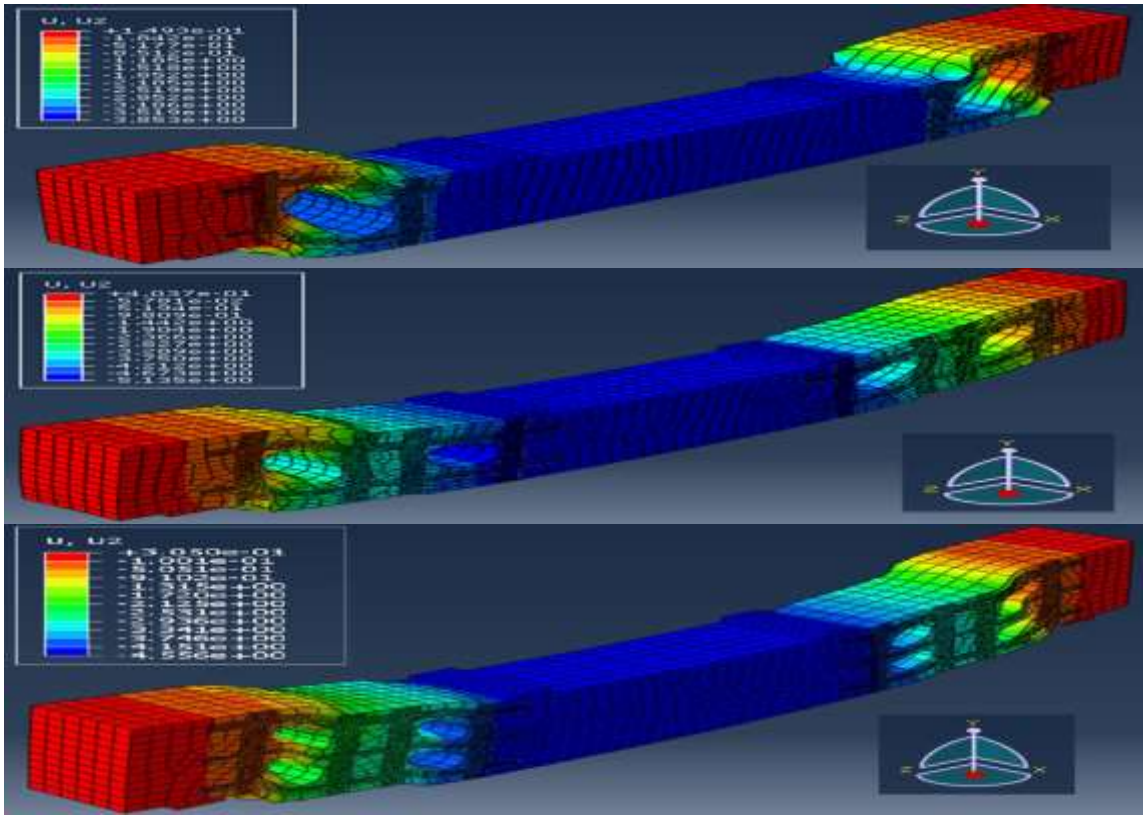

(b). beams with externally strengthening MD beam opening RCBCO,2,4, and8

Figure 13. contour plots from ABAQUS analyses for MD beams.

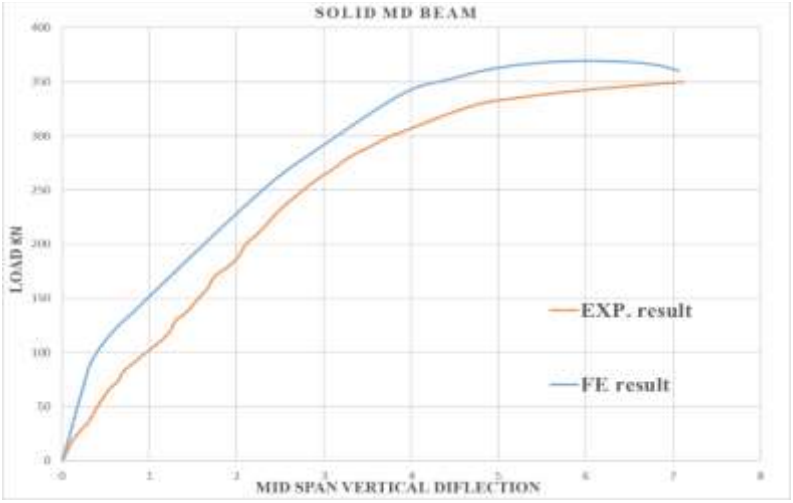

(a). solid MD beam

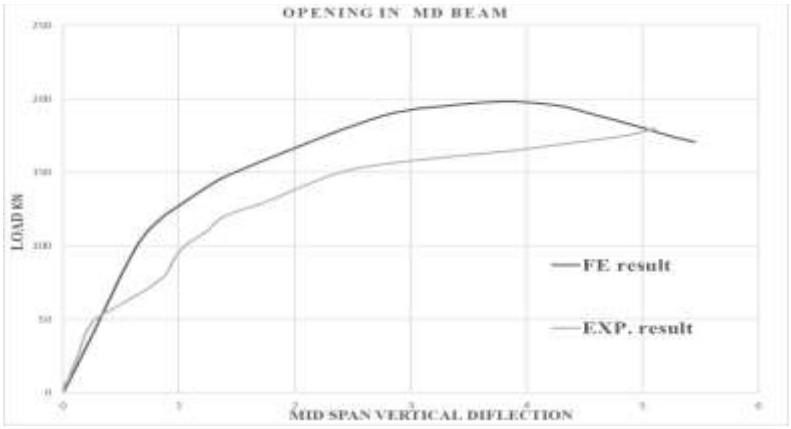

(b). Two circle opening RCBCO,2

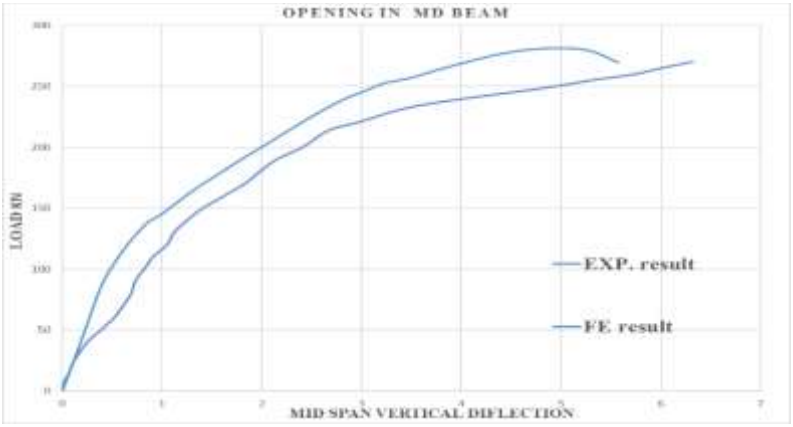

(b). Four circle opening RCBCO,4

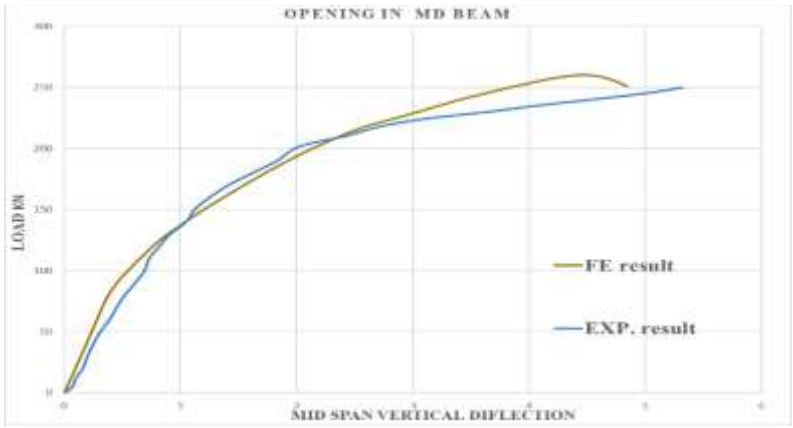

(b). Eight circle opening RCBCO,8

Figure 14. Load-deflection curves of FE and experiment MD beam result.

11. CONCLUSION

1. The FEM using the ABAQUS program was used to simulate rectangular MD beams with web openings and the result of FEM showed a stiffer behavior than the experiments test data.
2. The presence of the circular openings in the center of the load path (shear zone) had a considerable influence on the behavior of MD beams. It is obvious that the reducing in load

carrying capacity of beam with openings was 48%, whereas the deflection at 198 kN is 5.11 mm.

3. The presence of eight and four openings give a high strength than the two circles opening in spite of the equivalent area of the opening because of the higher depth of the top and bottom chord member for the eight and four openings and also the CFRP stretched for long-distance on the surface of the beam.
4. The ultimate loads from the experimental results less than the final loads from the FE analyses with differences (4.1 to 10.2 %) these are acceptable.
5. The FE/EXP results indicate good agreement between the experimental and FE results of maximum deflection. The ratio of FE ultimate deflection to the experimental ultimate deflection ranges from 0.74 (beam RCBOC,2) to 0.85 for (solid MD beam).
6. The failure load and maximum deflection predicated by FEM are quite close the actual test load and deflection.
7. The FE/EXP results indicate good agreement between the experimental and FE results. the ratio of FE ultimate load to the experimental ultimate load ranges from 1.04 (beambRCBOC,4 AND 8), to 1.1 (beam RCBOC,2).
8. The maximum deflection and failure load that resulted from the FEM close to the actual load and deflection test and give a good agreement between them.
9. The presence of the openings in the shear influence on the behavior of FE for MD beam. It is obvious that the decreasing percentage of the ultimate load carrying capacity of MD beam with openings ranging from (22.8 to 48.57%).

REFERENCES

- (PC200), S., 2014. High performance concrete superplasticizer. s.l.:s.n.
- Abaqus, C., 2016-2017. User's Manual. Abaqus analysis user's manual.
- Abdalla, H.,. 2003. Design against cracking at openings in reinforced concretebeams strengthened with composite sheets. Composite Structures, Volume 60, pp. 197-204.
- ACI 318, C., 2014. Building Code Requirement for Structural Concrete. Philadelphia: American Concrete Institute.
- Ahmed, A., 2014. Modeling of a reinforced concrete beam subjected to impact vibration using ABAQUS. INTERNATIONAL JOURNAL OF CIVIL AND STRUCTURAL ENGINEERING, 4(0976 – 4399), pp. 227-236.
- Al-Ahmed, D. A. H. A., 2016. Nonlinear Behavior of Self -Compacting Reinforced Concrete Two-Way Slabs with Central Square Opening under Uniformly Distributed Loads. Journal of Engineering, Volume 22, pp. 35-54.
- CFRP, S.-9., 2017. STITCHED UNIDIRECTIONAL CARBON FIBRE FABRIC, DESIGNED FOR STRUCTURAL STRENGTHENING APPLICATIONS AS PART OF THE SIKA® STRENGTHENING SYSTEM. Egypt: Version 01.01.
- Dr. Rafa'a Mahmood Abbas, H. J. S., 2015. Finite Element Investigation on Shear Lag in Composite Concrete-Steel Beams with Web Openings. Journal of Engineering, Volume 21.
- Hejazi, F., 2017. Simplified Damage Plasticity Model for Concrete. Structural Engineering International.

- IQ.S. No45, I. s., 1980. Natural aggregate used in concrete. Central Organization for Standardization and Quality Control.
- IQ.S.No40, I. s., 1984. Portland cement. Central Organization forStandardization and Quality Control.
- Jassim, N. Q., 2017. Enhancement of Behavior of ReinforcedConcrete Beams with Large OpeningsUsing Hybrid Sections. Al-Nahrain Journal for Engineering Sciences(NJES) , Volume 21, pp. 405-416.
- K. Senthil, A. G. a. S. S., 2018. Computation of stress-deformation of deep beam with openings using finite element method. Advances in Concrete Construction, 6(2287-531X), pp. 245-268.
- Mansur, M., 2006. DESIGN OF REINFORCED CONCRETE BEAMS WITH WEB OPENINGS.
- Maryam Abdul Jabbar Hassan, A. F. I., , 2019. Serviceability of Reinforced Concrete Gable Roof Beams with Openings under Static Loads. Engineering, Technology & Applied Science Research, Volume 9, pp. 4813-4817.
- Nahid Askarizadeh, M. R. M., 2017. Numerical Analysis of Carbon Fiber Reinforced Plastic (CFRP) Shear Walls and Steel Strips under Cyclic Loads Using Finite Element Method. Engineering, Technology & Applied Science Research, 7(2147-2155), pp. 2147-2155.
- S.C. Chin, N. S. a. M. N., 2012. Strengthening of RC Beams with Large Openings in Shear by CFRP Laminates:Experiment and 2D Nonlinear Finite Element Analysis. Research Journal of Applied Sciences, Engineering and Technology, pp. 1172-1180.
- Shammari, N. K. O. a. A. H., 23 2015. Response of Reinforced Concrete Beams with Multiple Web Openings to Static Load. Fourth Asia-Pacific Conference on FRP in Structures .
- Sherif, T. E. M. a. S., Jun. 2009. FRP composites for shear strengthening of reinforced concrete deep beams with openings. Composite Structures, Volume 89, pp. 60-69.